HHS Public Access

Author manuscript

J Vasc Res. Author manuscript; available in PMC 2018 January 18.

Published in final edited form as:

J Vasc Res. 2017 ; 54(1): 1–12. doi:10.1159/000454812.

Impaired mitochondrial respiration in large cerebral arteries of rats with type 2 diabetes

Ivan Merdzo, **Ibolya Rutkai**, **Venkata N. L. R. Sure**, **Catherine A. McNulty**, **Prasad V. G. Katakam**, and **David W. Busija**

Department of Pharmacology, Tulane University School of Medicine, New Orleans, LA, USA

Abstract

Mitochondrial dysfunction has been suggested as a potential underlying cause of pathological conditions associated with type 2 diabetes (T2DM). We have previously shown that mitochondrial respiration and mitochondrial protein levels were similar between the large cerebral arteries of insulin resistant Zucker obese rats and their lean controls. In the present study we extended our investigations into mitochondrial dynamics of the cerebral vasculature of 14 week old Zucker diabetic fatty obese rats (ZDFO) with early T2DM. Body weight and blood glucose levels were significantly higher in the ZDFO group, and basal mitochondrial respiration and proton leak were significantly decreased in the large cerebral arteries of the ZDFO rats compared with lean controls (ZDFL). The expression of mitochondrial proteins total MnSOD and VDAC were significantly lower in the cerebral microvessels, and the acetylated MnSOD levels were significantly reduced in large arteries of ZDFO group. Additionally, superoxide production was significantly increased in the microvessels of the ZDFO group. Despite evidence of increased oxidative stress in ZDFO, exogenous superoxide dismutase was not able to restore mitochondrial respiration in ZDFO rats. Our results show for the first time that mitochondrial respiration and proteins levels are compromised during the early stages of T2DM.

Keywords

type 2 diabetes; mitochondria; mitochondrial respiration; cerebral arteries; cerebral microvessels

Introduction

Diabetes is a global health problem, and type 2 diabetes mellitus (T2DM) accounts for over 90% of the cases. Approximately 9.3% of people in the United States have diabetes with the prevalence increasing dramatically [1]. Although diagnostic and therapeutic possibilities are advanced, diabetes is still a leading cause of renal failure, ischemic heart disease, blindness

Address for correspondence: Dr. Ivan Merdzo, Department of Pharmacology, Tulane University School of Medicine, 1430 Tulane Avenue, MC 8683, New Orleans, LA, 70112-2632, Phone: 504-988-2628, Fax: 504-988-5283, imerdzo@tulane.edu.

Author contributions: I.M. and D.W.B. conceived and designed the experiments; I.M., I.R., V.N.L.R.S., C.A.M, and P.V.G.K., performed experiments; I.M. and D.W.B. analyzed data; I.M. and D.W.B. interpreted experimental results; I.M. and D.W.B prepared figures; I.M. drafted manuscript; I.M., I.R., V.N.L.R.S., C.A.M, P.V.G.K., and D.W.B. edited and revised manuscript; I.M., I.R., V.N.L.R.S., C.A.M, P.V.G.K., and D.W.B. approved final version of manuscript.

Disclosure/Conflict of interest: None.

due to retinopathy, and limb amputations [2–4]. Insulin resistance is the key factor in the development of T2DM [5] and the role of mitochondria in the pathogenesis of insulin resistance and T2DM has been a topic of many studies in different tissues and cells [6]. Some studies have suggested mitochondrial dysfunction as a potential underlying cause of insulin resistance [7,8], whereas others have reported normal mitochondrial respiratory capacity [9,10] and content [9,11] in insulin resistant humans. A significant number of studies correlate impaired mitochondrial function with T2DM [6,12–15] but it is unknown whether mitochondrial dysfunction leads to insulin resistance and T2DM or vice versa. Our laboratory has previously shown that mitochondrial dependent vasodilatory responses are diminished in major cerebral arteries of the insulin resistant Zucker obese (ZO) rat [16–18] and that the cerebrovascular dysfunction of the ZO rat is mediated by oxidative stress [19]. We have also shown that local cortical microcirculatory responses to different blood flow stimulators were not altered in insulin resistant ZO rats compared with their lean controls [20]. Recently, we have shown that mitochondrial respiration as well as mitochondrial protein expression levels in cerebral arteries and microvessels of ZO rats were similar compared with the Zucker lean (ZL) controls [21]. These results were obtained on animals in the early stages of insulin resistance, therefore we extended these studies to investigate changes in mitochondrial energetics with the development of T2DM. We used Zucker diabetic fatty obese (ZDFMO) rats as a model of T2DM and Zucker diabetic fatty lean rats (ZDFL) as a control. We hypothesized that mitochondrial respiration and the expression of mitochondrial proteins would be decreased in the cerebral vasculature of ZDFO rats. We examined mitochondrial dynamics in the large cerebral arteries and cerebral microvessels from the parenchyma since disease states can influence various cerebral vascular segments differently. Therefore, we used freshly isolated large cerebral arteries to measure mitochondrial respiration and determined levels of mitochondrial proteins and superoxide in the isolated cerebral microvessels.

Materials and Methods

The animal use protocols were approved by the Institutional Animal Care and Use Committee (IACUC) of Tulane University School of Medicine and complied with the National Institutes of Health (NIH) guidelines. Animal care was provided by the Department of Comparative Medicine. We used 14 week old, male ZDFO and ZDFL rats from Charles River Laboratories (Wilmington, MA). Forty animals from each group were used; *n* represents number of individual measurements.

Zucker diabetic fatty rat model

The obese, male, Zucker diabetic fatty rat (ZDFO) maintained on a Purina 5008 diet exhibits obesity, insulin resistance, hyperinsulinemia, hyperglycemia, and T2DM beginning at 6–7 weeks of age. Glucose levels steadily increase until the age of 10–12 weeks and then are maintained at an average of approximately 27.8 mmol/L [22].

Blood glucose measurements

Blood samples were taken from the aorta while animals were deeply anesthetized. Blood glucose levels were measured using a glucometer (Contour next EZ glucometer, Bayer, Germany) and expressed in mmol/L as mean ± SEM.

Isolation of cerebral arteries and microvessels

Animals were decapitated after deep anesthesia via 5% isoflurane (VetOne, Boise, ID). Brains were removed and placed in ice-cold phosphate buffered saline (PBS). All procedures were done on ice or at 4°C as described previously [21]. Briefly, large cerebral arteries (anterior and middle cerebral, and basilar arteries) were isolated, cleaned, and used for mitochondrial respiration measurements. Then, cerebral microvessels were isolated. The cortex was homogenized, centrifuged at 1000 g for 10 min; the supernatant was discarded and the pellet was resuspended in 17.5% dextran (64–76 kDa, Sigma Aldrich, St. Louis, MO), passed through 300 μm mesh, and centrifuged at 4400 g for 15 min. The same steps were repeated with the resulting supernatant to increase the yield of microvessels. Finally, microvessel pellets from the previous two centrifugations were resuspended together in 17.5% dextran, centrifuged, and the resulting pellet was passed through a 70 μm nylon mesh. Captured microvessels were washed with PBS, collected, and used for western blotting. This microvessels isolation method was validated via immunohistochemistry [21].

Mitochondrial respiration measurement

We used the Seahorse Bioscience (currently Agilant Corporation) XFe24 extracellular flux analyzer to measure mitochondrial oxygen consumption rate (OCR), an indicator of mitochondrial respiration [23–25]. To establish the validity and reproducibility of our methodology, we performed separate determinations of mitochondrial respiration on different groups of rats during experiments performed approximately two months apart. We used freshly isolated large cerebral arteries for these measurements as described previously [21,26]. Briefly, we placed the arteries into the wells of the XF24 islet capture microplate (#101122-100, Seahorse Bioscience, Corporate US Headquarters, MA). The wells were then filled with the XF assay medium (#102365-100, Seahorse Bioscience, MA) containing 5.0 mM/L glucose and 2 mM/L pyruvate and the plates were kept in a non-CO_2 incubator at 37°C for 20 min. Afterward, plates were placed into the Seahorse Bioscience analyzer where oxygen and hydrogen ion sensitive fluorophores repeatedly allowed determination of the oxygen and hydrogen concentration in the medium surrounding the arteries, thus calculating OCR. The assay protocol consisted of eight cycles of baseline measurements followed by five cycles for each treatment. After baseline measurements, the plates were sequentially exposed to 2μM/L oligomycin, 1μM/L carbonyl cyanide 4-(trifluoromethoxy) phenylhydrazone (FCCP), and 1.5 μM/L antimycin plus 1.5 μM/L rotenone (A/R) to determine levels of different components of mitochondrial respiration (Figure 1). Two sample groups were analyzed: the ZDFO and ZDFL. Protein concentration, (Pierce bicinchoninic acid [BCA] protein assay kit, Thermo Scientific, Rockford, IL), was used to normalize OCR data, and values were expressed in pM/min/μg. After normalization, a series of calculations were performed using OCR data to determine various components of mitochondrial (basal respiration, proton leak, maximal respiration, and spare respiratory

capacity) and non-mitochondrial respiration. The same approach was used in the presence of a superoxide scavenger, polyethylene glycol-superoxide dismutase (PEG-SOD, 200 units/ml) (Creative Enzymes, Shirley, NY).

Electron spin resonance studies

Electron spin resonance (ESR) spectroscopy was used to determine levels of superoxide in the cerebral microvessels of the ZDFL and ZDFO rats, as described previously [17,21]. Briefly, the 1-hydroxy-3-methoxycarbonyl-2,2,5,5-tetramethyl-pyrrolidine (CMH) spin probe was used to measure superoxide production in the freshly isolated cerebral microvessels. Diethyldithiocarbamate (DETC; 2.5 μmol/L) and deferoxamine (25 μmol/L) were dissolved under nitrogen gas bubbling in ice-cold modified Krebs-Hepes (KH) buffer. Microvessels were then placed in a microtube containing 200 μmol/L CMH solution of KH buffer with deferoxamine and DETC, and the samples were incubated for 60 min at 37°C, placed into the barrel of 1 ml syringe, and frozen in liquid nitrogen. When samples were ready for measurement, the frozen column of microvessels was placed into a finger dewar (Noxygen Science Transfer & Diagnostics GmbH, Elzach, Germany) containing liquid nitrogen. The finger dewar was placed into the measuring cavity of a benchtop X-band EMX series ESR spectrometer (Bruker Biospin GmbH, Karlsruhe, Germany) and ESR spectra were obtained. Time-dependent formation of ROS was determined using the following ESR settings: center field, 1.99 g; microwave power, 20 mW; modulation amplitude, 2 G; sweep time, 10 s; number of scans, 10; field sweep, 60 G. The measurements of amplitude of the peak and through for each ESR spectrum was normalized to the protein concentrations of the microvessel samples and expressed in arbitrary units.

Western blot analysis

Proteins were harvested as described previously [17,21,26]. Briefly, isolated large cerebral arteries and microvessels were homogenized in ice-cold NP40 lysis buffer (Invitrogen, Frederick, MD) supplemented with proteinase inhibitor cocktail (Cat No. P8340; Sigma Aldrich, St. Louis, MO) and phosphatase inhibitor cocktail (Cat No. P2850; Sigma Aldrich, St. Louis, MO) and then centrifuged and the supernatant was analyzed. Pierce BCA protein assay (Thermo Scientific, Rockford, IL) was used to determine protein concentration. We then separated protein samples using gel electrophoresis on a 4–20% SDS-PAGE gradient gel. Proteins were transferred onto a polyvinylidene difluoride membrane, blocked with casein blocking buffer (#92740200, Li-cor, Lincoln, NE), washed, and incubated overnight with primary antibodies in casein blocking buffer at 4°C. The following primary antibodies for mitochondrial and non-mitochondrial proteins were used: Anti-Complex II Fp subunit I at 1:1000 dilution (70 KDa; #459200, Invitrogen, Frederick, MD); Anti-Complex III Subunit I core at 1:1000 dilution (53 KDa; #459140, Invitrogen, Frederick, MD); ATP synthase Complex V subunit alpha at 1:500 dilution (50 KDa; #459240, Invitrogen, Frederick, MD); anti-VDAC at 1:1000 dilution to detect the endogenous levels of total VDAC (32 KDa; #4866S, Cell Signaling Technology, Danvers, MA); total endothelial NOS (eNOS) at 1:500 dilution (140 kDa; no. 610297, BD Transduction Laboratories, San Jose, CA) and its Ser^{1176}phosphorylated form (peNOS) at 1:500 dilution (140 kDa; no. 9571, Cell Signaling Technology, Danvers, MA); total dynamin-related protein-1 (tDRP) at 1:1000 dilution (no. 611112, BD Transduction, San Jose, CA) and its Ser^{616}-phosphorylated form (pDRP) at

1:1,000 dilution (no. 3455, Cell Signaling Technology, Danvers, MA); total anti-manganese superoxide dismutase (total MnSOD) aa114–220 at 1:5000 (25 KDa; #611581, BD Transduction Laboratories, San Jose, CA); and its acetylated form anti-SOD2 (acetyl K68) (Acetylated MnSOD) at 1:500 dilution (24 kD, #ab137037, Abcam, Cambridge, MA). Loading control was β-actin at 1:5000 dilution (42 KDa; #A5441, Sigma Aldrich, St. Louis, MO). After incubation with the primary antibody, membranes were washed and incubated at room temperature for 90 min in 1%BSA-TBST with secondary goat anti-rabbit IgG at 1:2500 dilution (#7074S, Cell Signaling Technology, Danvers, MA) or goat anti-mouse IgG at 1:5000 dilution (#7076P2, Cell Signaling Technology, Danvers, MA). Immunobands were visualized using chemiluminescence (LumiGLO, Gaithersburg, MD) and autoradiography. Then, immunobands were scanned and analyzed using ImageJ software. We quantified the optical density of each band and normalized it to the intensity of the corresponding β-actin band.

Data analysis and statistics

Results were expressed as mean ± SE; *n* indicates the number of independent measurements. Data were analyzed by GraphPad Prism software, version 5.03 (GraphPad Software Inc., San Diego, CA) using unpaired t-test. A $P < 0.05$ was considered as statistically significant.

Results

Animal weight and blood glucose levels

The ZDFO group exhibited both significantly higher blood glucose values (26.33 ± 1.56 mmol/L vs. 9.18 ± 0.46 mmol/L, n = 40, $P < 0.05$) (Figure 2A), and body weight (347.2 ± 10.18 g vs. 320.4 ± 3.9 g, n = 40, $P < 0.05$) (Figure 2B) compared with their lean controls.

Mitochondrial respiration measurements

Mitochondrial respiration studies were performed twice, separated by approximately two months (Figure 3A and 3B, respectively), on two separate groups of 14 week old rats. Eight independent Seahorse experiments, with 20 animals in each group, confirmed the high level of reproducibility and validated our optimized methods to adopt Seahorse Bioscience Extracellular Flux analyzer to evaluate the bioenergetics of freshly isolated cerebral arteries. The mitochondrial respiration profile of the large cerebral arteries with the merged results from the first two sets of experiments is shown in Figure 3C. Individual components of mitochondrial (basal respiration, ATP production, spare capacity, and proton leak) and non-mitochondrial respiration are shown for both sets of experiments (Figure 4) as well as for the merged results (Figure 5). Basal respiration was significantly higher in ZDFL compared with ZDFO (181.4 ± 10.93 pM/min/μg protein vs. 129.7 ± 8.211 pM/min/μg protein; $n = 59$, $P < 0.05$) (Figures 4B and 5B) and proton leak was also significantly higher in ZDFL compared with ZDFO (149.3 ± 10.41 pM/min/μg protein vs. 100.3 ± 7.56 pM/min/μg protein; $n = 59$, $P < 0.05$) (Figures 4E and 5E). Other components of mitochondrial and non-mitochondrial respiration were not significantly different between the groups (Figures 4 and 5).

Protein expression

The expression of proteins associated with mitochondrial function (total MnSOD and VDAC) was significantly lower in the microvessels of ZDFO compared with ZDFL (90.35 ± 9.13% vs. 123.1 ± 12.77%, $n = 13$, $P < 0.05$; and 23.63 ± 2.62% vs. 30.54 ± 2.07%, $n = 12$, $P < 0.05$; respectively) (Figure 6B and 6C). Levels of the other mitochondrial and non-mitochondrial proteins (pDRP, tDRP, peNOS, teNOS; $n = 12–16$ per group) were not significantly different between the groups (Figure 7).

The large cerebral arteries showed higher levels of acetylated MnSOD in ZDFL compared with ZDFO (89.72 ± 3.17% vs. 52.23 ± 6.01%, $n = 12$, $P < 0.05$) (Figure 8A). Levels of the other mitochondrial and non-mitochondrial proteins (pDRP, tDRP, peNOS, teNOS; $n = 12–16$ per group) did not show a significant difference between the groups (Figure 9).

Superoxide production in cerebral microvessels

The normalized amplitude of the characteristic ESR signal was significantly higher in the microvessels from ZDFO compared to ZDFL (2355 ± 628 vs. 208 ± 48, $n = 10$, $P < 0.05$) (Figure 10A). Thus, superoxide levels in ZDFO microvessels are ten-fold higher than in ZDFL animals.

Mitochondrial respiration measurements in the presence of a superoxide scavenger

The PEG-SOD treatment did not have a significant effect on mitochondrial respiration and was unable to restore the mitochondrial respiration levels in ZDFO (Figure 10B).

Discussion

We have directly determined mitochondrial respiration in large cerebral arteries of male diabetic ZDFO rats for the first time. Our major, new findings include the following: 1) Basal mitochondrial respiration is significantly decreased in the large cerebral arteries of ZDFO compared with ZDFL rats; 2) Proton leak is significantly lower in the large cerebral arteries of ZDFO compared with ZDFL; 3) Expression of mitochondrial proteins (VDAC and total MnSOD) was significantly reduced in the microvessels, and acetylated MnSOD was significantly reduced in the large cerebral arteries of ZDFO compared with the ZDFL. These findings indicate that deterioration of mitochondrial function in the cerebral vasculature starts during early T2DM.

Our laboratory pioneered the use of the Seahorse Bioscience XFe24 extracellular flux analyzer to determine mitochondrial respiration in freshly isolated large cerebral arteries. Due to factors such as intra-animal variation, trauma and delays during removal of the arteries, and other intangible factors related to any experiment, we felt it to be important to examine the reproducibility of our results. In the current study, we demonstrated that we could achieve virtually identical measurements of mitochondrial respiration in large arteries from ZDFO and ZDFL rats of the same age in experiments separated by two months. Although not specifically detailed in this manuscript, we find similar reproducibility of results with western blotting.

Although the role of mitochondria in the pathogenesis of insulin resistance and T2DM has been the subject of many studies, additional information is necessary to further elucidate the exact mechanism in these processes. Considering the conflicting reports regarding the role of mitochondria in the development of insulin resistance and T2DM [6–11,15] the question that remains to be answered is whether the impairment of mitochondrial function causes insulin resistance and T2DM or it derives from it. It is important to note that mitochondrial function has different implications regarding diabetes in different tissues and cells [6] and that the cited studies were performed on different samples and in different stages of the disease. Different tissues and cells also exhibit different mitochondrial morphology in certain conditions [27–29]. We have found that even within the same population of vascular cells during insulin resistance, one aspect of mitochondrial function is altered (arterial dilation to mitochondrial depolarizing agents) while others aspects are unchanged (total cerebral artery mitochondrial respiration and protein levels) [18,19,21]. One study argues that if mitochondrial impairment leads to T2DM, it should be present in the early stages of insulin resistance, but the investigators found normal mitochondrial respiration and mitochondrial content in these early stages [9].

Previous studies from our lab have also focused on the early stages of insulin resistance in the absence of diabetes and found decreased vasodilation of the insulin resistant rat's cerebral arteries that was mediated by mitochondrial depolarization [16,17]. Excess production of reactive oxygen species (ROS) plays a key role in reduced vasodilatory responses in cerebral arteries of the insulin resistant rats since pretreatment with superoxide-dismutase restored all of the examined dilator responses [19,30]. We have also shown that rosuvastatin improves cerebrovascular function during insulin resistance by inhibiting NAD(P)H oxidase dependent superoxide production [31]. This finding implies that irreversible changes have not yet occurred in the cerebral vasculature this early in the disease progression. Although functional tests showed lower responses in the cerebral arteries of insulin resistant rats, microcirculatory responses to different pharmacological and physiological stimuli were similar between the insulin resistant and the control groups [20].

Considering that impaired cerebrovascular responses to mitochondrial depolarizing agents occur during insulin resistance, we conducted further experiments to directly measure mitochondrial respiration in the cerebral arteries of insulin resistant rats and found very similar respiration profiles and similar mitochondrial protein expression between the insulin resistant and control group [21]. However, we found significantly higher superoxide levels in cerebral microvessels which is consistent with previous findings in which oxidative stress plays a significant role even early in the development of insulin resistance and T2DM. It has been reported that high glucose levels during diabetes lead to increase in ROS production in cerebral vascular endothelium [32] by creating excess electron donors that generate an increase in mitochondrial membrane potential. High mitochondrial membrane potential inhibits complex III of the respiratory chain. Also, it increases the half-life of free radical intermediate of coenzyme q, necessary for reduction of oxygen to superoxide. Thus, this sequence of events leads to abnormal ROS levels [33]. Increased levels of free radicals can then target proteins, lipids, polysaccharides, and DNA, causing mitochondrial respiration changes. In the present study, we have shown that basal mitochondrial respiration in the cerebral arteries decreases when diabetes is fully developed which suggests that this is a

consequence of T2DM. We have also shown that the cerebral arteries of the ZDFO rats have significantly higher levels of proton leak. Proton leak indicates the flow of the proton gradient across the inner mitochondrial membrane that was not used to drive the ATP synthase. It can be affected by ROS generation, mitochondrial membrane composition [34,35], and uncoupling of proteins (UCPs) [36]. Many important roles of the UCPs have been discussed including protection of the cells from the oxidative stress damage and mitigation of insulin secretion [37]. Increased proton leak in ZDFO arteries may be a compensatory response to increased ROS generation.

A novel finding was that levels of total MnSOD, located in the matrix, and VDAC, located in the outer membrane, were significantly lower in the cerebral microvessels of the ZDFO compared with the control group. Manganese SOD and VDAC are considered key mitochondrial proteins involved in responses to stress and apoptosis. Both of these proteins are encoded by nuclear DNA and incorporated into the mitochondria after being produced in the cytosol. While the other mitochondrial proteins examined were not different in the two groups, the reductions in total MnSOD and VDAC show that structural aspects of mitochondria are beginning to be adversely affected in parenchymal blood vessels at an early stage of T2D. Although total levels of total MnSOD in large, surface arteries were similar between the groups, levels of acetylated MnSOD, which represents a less active form of the enzyme, were reduced in large arteries of ZDFO rats. Reversible acetylation is an important regulating mechanism in the oxidative stress protection. Acetylation of mitochondrial proteins plays a role in maintaining and regulating mitochondrial ROS levels. The *Sirt3* gene appears to be a crucial element. *Sirt3* serves as main mitochondrial deacetylase and decreases MnSOD acetylation and thereby increases MnSOD activity [38]. These results indicate that the SOD capacity of this enzyme is enhanced in large arteries of diabetic rats, possibly in response to oxidative stress. These findings of functional, but not structural, changes in mitochondria of large cerebral arteries are consistent with studies of dilator responses of insulin resistant and diabetic animals, where responsiveness is restored quickly in the presence of ROS scavengers. Although the response mode of MnSOD to diabetes differs in large, surface arteries compared with parenchymal microvessels and cerebral vascular segments that are subjected to different environmental stimuli, the common feature is that a major ROS scavenging enzyme is substantially affected by even early T2DM. As we have observed in cerebral microvessels, increased superoxide production may represent the initiating event. It has been reported that downregulation of VDAC in coronary endothelial cells of type 1 diabetic mice decreases mitochondrial superoxide generation [39]. Our finding of lower VDAC levels in the cerebral microvessels of the ZDFO rats might represent another compensatory mechanism, in addition to altered MnSOD dynamics, to minimize the detrimental consequences of increased oxidative stress in T2DM. Further studies are required to elucidate the roles of MnSOD and VDAC and other mitochondrial proteins during disease states.

There were some limitations to our study. Only male rats were used. Future studies in female rats or mice as well as in older rodents with more established T2DM are planned. The mitochondrial respiration studies were only performed on large arteries because of the insufficient mass of the microvessels and the technical limitations of the Seahorse Bioscience analyzer. We are exploring ways to conduct similar determinations on

microvessels. Finally, we have not yet been able to differentiate the cell-specific mitochondrial responses using large cerebral arteries and microvessels. In future studies we will explore individual responses of cell types by culturing endothelial and vascular smooth muscle cells.

The complex interactions between insulin resistance, T2DM, and mitochondrial function still require additional studies to elucidate all of the underlying mechanisms. The functional characteristics of the cerebral vasculature seem to be impaired even in the early stages of insulin resistance. However, decrement in the mitochondrial respiration and certain mitochondrial proteins in the cerebral vessels appear to be a consequence of the disease rather than the underlying cause.

Acknowledgments

We thank Nancy Busija, M.A. for editorial assistance. We thank Dana Liu for technical help.

Sources of Funding: This work was supported by National Institutes of Health grants (DWB: HL-077731 and HL093554; PVK: NS094834) American Heart Association Greater Southeast Affiliate postdoctoral fellowship grant (IR: 15POST23040005), American Heart Association Greater Southeast Affiliate predoctoral fellowship grant (VNS: 16PRE31450006), American Heart Association National Center Scientist Development Grant (PVK: 14SDG20490359), and Louisiana Board of Regents Support Fund-Research Competitiveness Subprogram (PVK: LEQSF(2014–17)-RD-A-11). This research was also supported by the Louisiana Board of Regents Endowed Chairs for Eminent Scholars program (DWB).

References

1. Centers for Disease Control and Prevention. National Diabetes Statistics Report: Estimates of Diabetes and Its Burden in the United States, 2014. Atlanta, GA: US Department of Health and Human Services; 2014.
2. Deshpande AD, Harris-Hayes M, Schootman M. Epidemiology of diabetes and diabetes-related complications. Phys Ther. 2008; 88:1254–1264. [PubMed: 18801858]
3. Ahola AJ, Saraheimo M, Forsblom C, Hietala K, Sintonen H, Groop PH. Health-related quality of life in patients with type 1 diabetes--association with diabetic complications (the FinnDiane Study). Nephrology, dialysis, transplantation : official publication of the European Dialysis and Transplant Association - European Renal Association. 2010; 25:1903–1908.
4. Martin CL, Albers J, Herman WH, Cleary P, Waberski B, Greene DA, Stevens MJ, Feldman EL. Neuropathy among the diabetes control and complications trial cohort 8 years after trial completion. Diabetes care. 2006; 29:340–344. [PubMed: 16443884]
5. Alberti KG, Zimmet P, Shaw J. Metabolic syndrome--a new world-wide definition. A Consensus Statement from the International Diabetes Federation. Diabetic medicine : a journal of the British Diabetic Association. 2006; 23:469–480. [PubMed: 16681555]
6. Sivitz WI, Yorek MA. Mitochondrial dysfunction in diabetes: from molecular mechanisms to functional significance and therapeutic opportunities. Antioxidants & redox signaling. 2010; 12:537–577. [PubMed: 19650713]
7. Kelley DE, He J, Menshikova EV, Ritov VB. Dysfunction of mitochondria in human skeletal muscle in type 2 diabetes. Diabetes. 2002; 51:2944–2950. [PubMed: 12351431]
8. Ritov VB, Menshikova EV, He J, Ferrell RE, Goodpaster BH, Kelley DE. Deficiency of subsarcolemmal mitochondria in obesity and type 2 diabetes. Diabetes. 2005; 54:8–14. [PubMed: 15616005]
9. Fisher-Wellman KH, Weber TM, Cathey BL, Brophy PM, Gilliam LA, Kane CL, Maples JM, Gavin TP, Houmard JA, Neufer PD. Mitochondrial respiratory capacity and content are normal in young insulin-resistant obese humans. Diabetes. 2014; 63:132–141. [PubMed: 23974920]

10. Lefort N, Glancy B, Bowen B, Willis WT, Bailowitz Z, De Filippis EA, Brophy C, Meyer C, Hojlund K, Yi Z, Mandarino LJ. Increased reactive oxygen species production and lower abundance of complex I subunits and carnitine palmitoyltransferase 1B protein despite normal mitochondrial respiration in insulin-resistant human skeletal muscle. Diabetes. 2010; 59:2444–2452. [PubMed: 20682693]
11. Karakelides H, Irving BA, Short KR, O'Brien P, Nair KS. Age, obesity, and sex effects on insulin sensitivity and skeletal muscle mitochondrial function. Diabetes. 2010; 59:89–97. [PubMed: 19833885]
12. Jeong EM, Chung J, Liu H, Go Y, Gladstein S, Farzaneh-Far A, Lewandowski ED, Dudley SC Jr. Role of Mitochondrial Oxidative Stress in Glucose Tolerance, Insulin Resistance, and Cardiac Diastolic Dysfunction. Journal of the American Heart Association. 2016; 5
13. Choo HJ, Kim JH, Kwon OB, Lee CS, Mun JY, Han SS, Yoon YS, Yoon G, Choi KM, Ko YG. Mitochondria are impaired in the adipocytes of type 2 diabetic mice. Diabetologia. 2006; 49:784–791. [PubMed: 16501941]
14. Petersen KF, Dufour S, Befroy D, Garcia R, Shulman GI. Impaired mitochondrial activity in the insulin-resistant offspring of patients with type 2 diabetes. The New England journal of medicine. 2004; 350:664–671. [PubMed: 14960743]
15. Petersen KF, Befroy D, Dufour S, Dziura J, Ariyan C, Rothman DL, DiPietro L, Cline GW, Shulman GI. Mitochondrial dysfunction in the elderly: possible role in insulin resistance. Science (New York, NY). 2003; 300:1140–1142.
16. Katakam PV, Domoki F, Snipes JA, Busija AR, Jarajapu YP, Busija DW. Impaired mitochondria-dependent vasodilation in cerebral arteries of Zucker obese rats with insulin resistance. American journal of physiology Regulatory, integrative and comparative physiology. 2009; 296:R289–298.
17. Katakam PV, Gordon AO, Sure VN, Rutkai I, Busija DW. Diversity of mitochondria-dependent dilator mechanisms in vascular smooth muscle of cerebral arteries from normal and insulin-resistant rats. American journal of physiology Heart and circulatory physiology. 2014; 307:H493–503. [PubMed: 24929852]
18. Busija DW, Rutkai I, Dutta S, Katakam PV. Role of Mitochondria in Cerebral Vascular Function: Energy Production, Cellular Protection, and Regulation of Vascular Tone. Comprehensive Physiology. 2016; 6:1529–1548. [PubMed: 27347901]
19. Erdos B, Snipes JA, Miller AW, Busija DW. Cerebrovascular dysfunction in Zucker obese rats is mediated by oxidative stress and protein kinase C. Diabetes. 2004; 53:1352–1359. [PubMed: 15111506]
20. Institoris A, Lenti L, Domoki F, Wappler E, Gaspar T, Katakam PV, Bari F, Busija DW. Cerebral microcirculatory responses of insulin-resistant rats are preserved to physiological and pharmacological stimuli. Microcirculation (New York, NY: 1994). 2012; 19:749–756.
21. Merdzo I, Rutkai I, Tokes T, Sure VN, Katakam PV, Busija DW. The Mitochondrial Function of the Cerebral Vasculature in Insulin Resistant Zucker Obese Rats. American journal of physiology Heart and circulatory physiology. 2016 ajpheart.00964.02015.
22. Shafrir, E. Animal Models of Diabetes: Frontiers in Research. 2. Boca Raton: CRC press; 2007.
23. Brand MD, Nicholls DG. Assessing mitochondrial dysfunction in cells. The Biochemical journal. 2011; 435:297–312. [PubMed: 21726199]
24. Gerencser AA, Chinopoulos C, Birket MJ, Jastroch M, Vitelli C, Nicholls DG, Brand MD. Quantitative measurement of mitochondrial membrane potential in cultured cells: calcium-induced de- and hyperpolarization of neuronal mitochondria. The Journal of physiology. 2012; 590:2845–2871. [PubMed: 22495585]
25. Hill BG, Benavides GA, Lancaster JR Jr, Ballinger S, Dell'Italia L, Jianhua Z, Darley-Usmar VM. Integration of cellular bioenergetics with mitochondrial quality control and autophagy. Biological chemistry. 2012; 393:1485–1512. [PubMed: 23092819]
26. Rutkai I, Dutta S, Katakam PV, Busija DW. Dynamics of Enhanced Mitochondrial Respiration in Female Compared with Male Rat Cerebral Arteries. American journal of physiology Heart and circulatory physiology. 2015 ajpheart.00231.02015.

27. Chalmers S, Saunter CD, Girkin JM, McCarron JG. Flicker-assisted localization microscopy reveals altered mitochondrial architecture in hypertension. Scientific reports. 2015; 5:16875. [PubMed: 26593883]

28. Ryan J, Dasgupta A, Huston J, Chen KH, Archer SL. Mitochondrial dynamics in pulmonary arterial hypertension. Journal of molecular medicine (Berlin, Germany). 2015; 93:229–242.

29. Marsboom G, Toth PT, Ryan JJ, Hong Z, Wu X, Fang YH, Thenappan T, Piao L, Zhang HJ, Pogoriler J, Chen Y, Morrow E, Weir EK, Rehman J, Archer SL. Dynamin-related protein 1-mediated mitochondrial mitotic fission permits hyperproliferation of vascular smooth muscle cells and offers a novel therapeutic target in pulmonary hypertension. Circulation research. 2012; 110:1484–1497. [PubMed: 22511751]

30. Erdos B, Simandle SA, Snipes JA, Miller AW, Busija DW. Potassium channel dysfunction in cerebral arteries of insulin-resistant rats is mediated by reactive oxygen species. Stroke; a journal of cerebral circulation. 2004; 35:964–969.

31. Erdos B, Snipes JA, Tulbert CD, Katakam P, Miller AW, Busija DW. Rosuvastatin improves cerebrovascular function in Zucker obese rats by inhibiting NAD(P)H oxidase-dependent superoxide production. American journal of physiology Heart and circulatory physiology. 2006; 290:H1264–1270. [PubMed: 16284235]

32. Carvalho C, Katz PS, Dutta S, Katakam PV, Moreira PI, Busija DW. Increased susceptibility to amyloid-beta toxicity in rat brain microvascular endothelial cells under hyperglycemic conditions. Journal of Alzheimer's disease : JAD. 2014; 38:75–83. [PubMed: 23948922]

33. Shah GN, Morofuji Y, Banks WA, Price TO. High glucose-induced mitochondrial respiration and reactive oxygen species in mouse cerebral pericytes is reversed by pharmacological inhibition of mitochondrial carbonic anhydrases: Implications for cerebral microvascular disease in diabetes. Biochemical and biophysical research communications. 2013; 440:354–358. [PubMed: 24076121]

34. Brand MD, Hafner RP, Brown GC. Control of respiration in non-phosphorylating mitochondria is shared between the proton leak and the respiratory chain. The Biochemical journal. 1988; 255:535–539. [PubMed: 2849419]

35. Rolfe DF, Brown GC. Cellular energy utilization and molecular origin of standard metabolic rate in mammals. Physiological reviews. 1997; 77:731–758. [PubMed: 9234964]

36. Busiello RA, Savarese S, Lombardi A. Mitochondrial uncoupling proteins and energy metabolism. Frontiers in physiology. 2015; 6:36. [PubMed: 25713540]

37. Brand MD, Esteves TC. Physiological functions of the mitochondrial uncoupling proteins UCP2 and UCP3. Cell metabolism. 2005; 2:85–93. [PubMed: 16098826]

38. Ozden O, Park SH, Kim HS, Jiang H, Coleman MC, Spitz DR, Gius D. Acetylation of MnSOD directs enzymatic activity responding to cellular nutrient status or oxidative stress. Aging. 2011; 3:102–107. [PubMed: 21386137]

39. Sasaki K, Donthamsetty R, Heldak M, Cho YE, Scott BT, Makino A. VDAC: old protein with new roles in diabetes. American journal of physiology Cell physiology. 2012; 303:C1055–1060. [PubMed: 22972802]

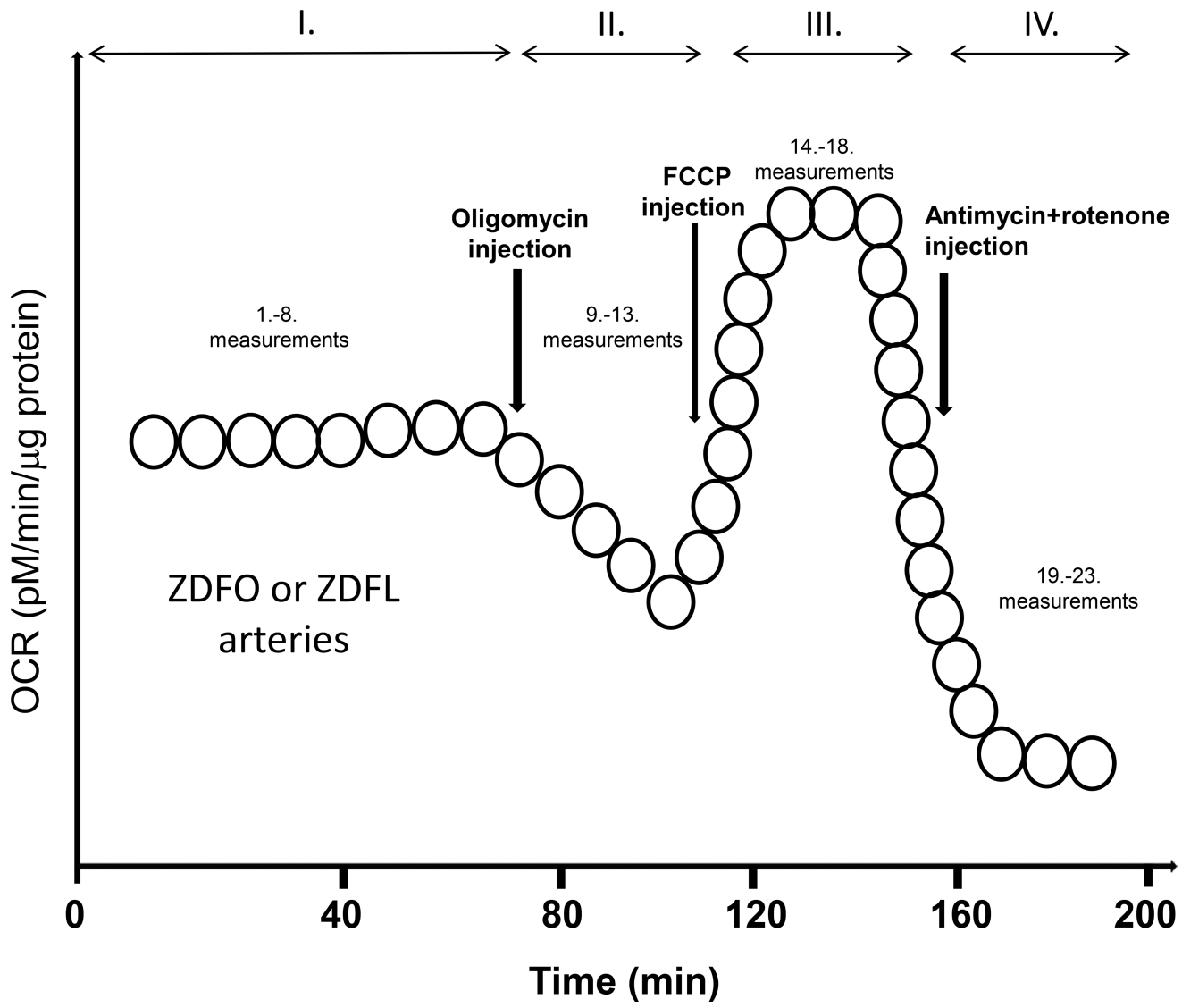

Figure 1.

Schematic illustration of the Seahorse experiment protocol. Roman numerals show different measurement cycles. Time points of different drug administration are marked with vertical arrows and resulting changes in OCR, expressed in pM/µg protein, are shown.

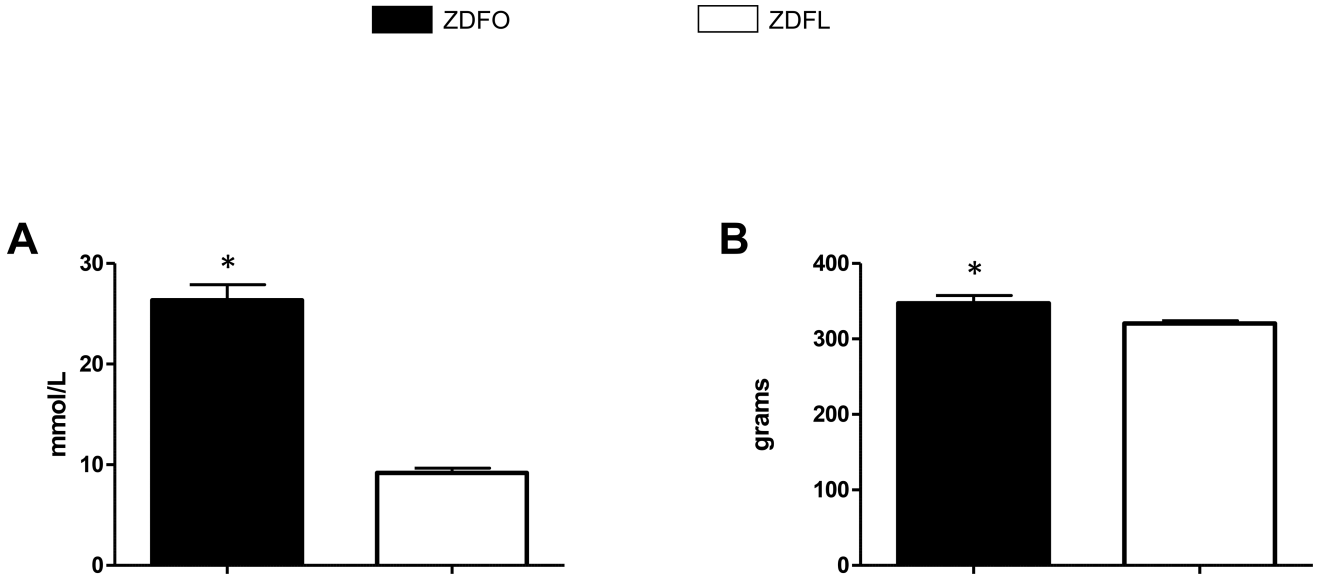

Figure 2. Blood glucose levels and weight of Zucker diabetic fatty lean (ZDFL) and obese rats (ZDFO)

(A) Blood glucose levels, assessed by the random blood glucose test, were significantly higher in ZDFO group. $n = 40$, * $P < 0.05$ (ZDFL vs. ZDFO). **(B)** ZDFO rats exhibited significantly higher body weight compared with the lean controls. $n = 40$, * $P < 0.05$ (ZDFL vs. ZDFO).

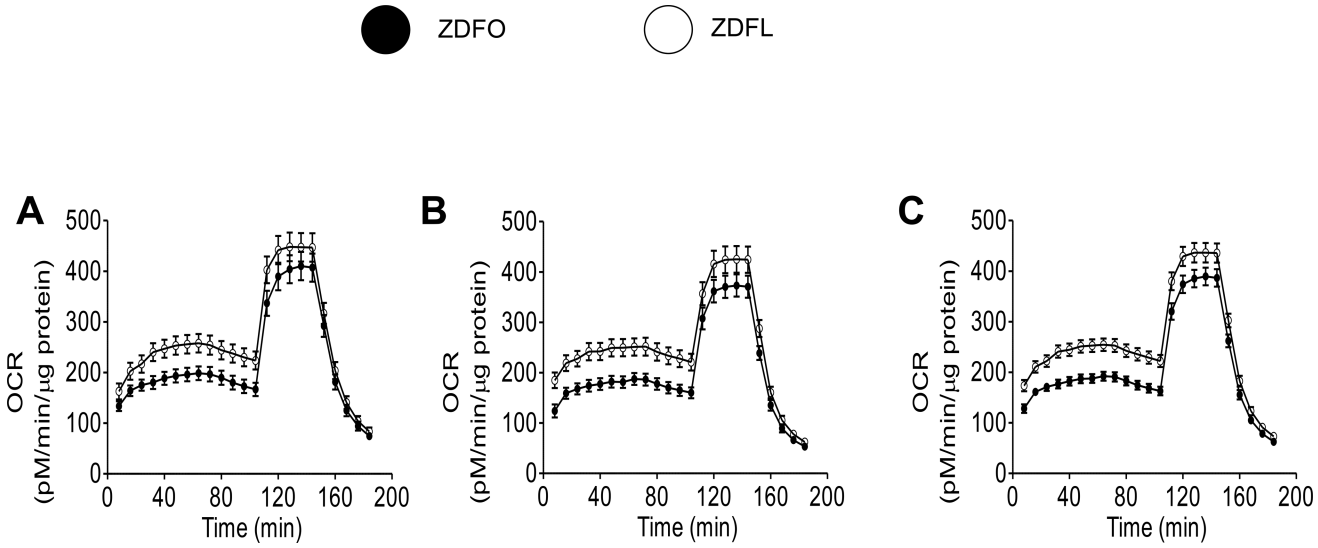

Figure 3. Mitochondrial respiration profile of large cerebral arteries from ZDFL and ZDFO rats

(A) First set of experiments. **(B)** Second set of experiments. **(C)** Merged results from both sets of experiments. Animals represented in A and B represent two groups of rats of the same age but in experiments separated by approximately two months. Data are expressed as mean ± SE; $n = 23$ per group.

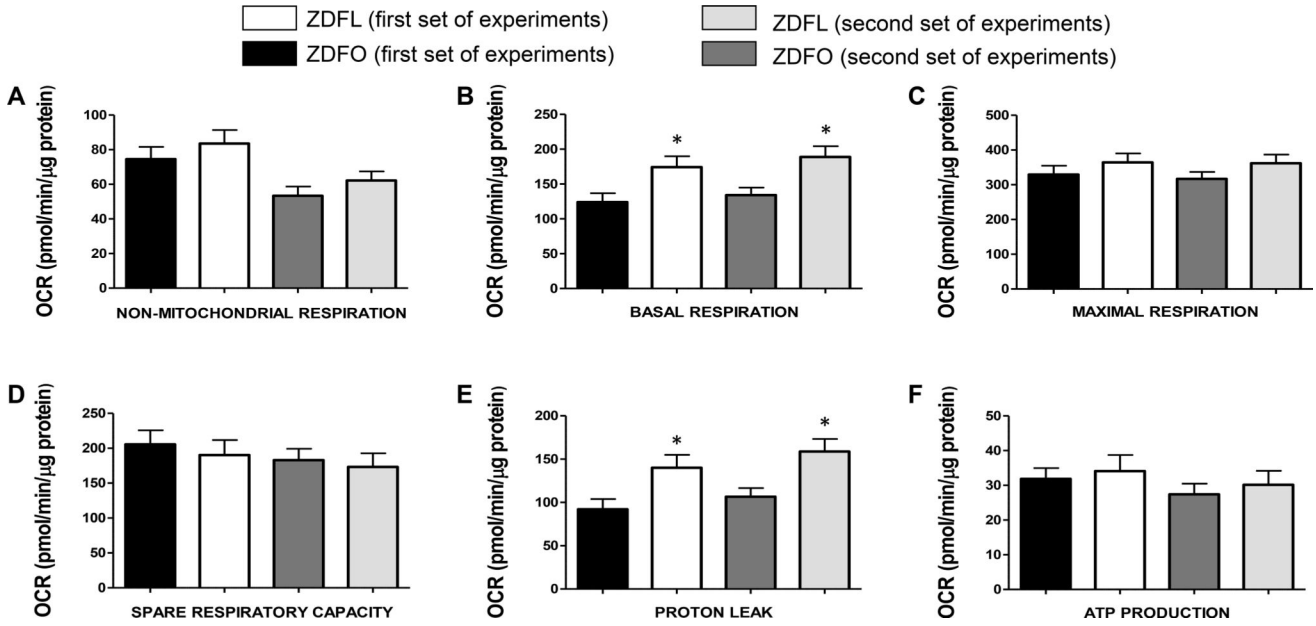

Figure 4. Mitochondrial respiration components of the large cerebral arteries for two individual sets of experiments

Mitochondrial bioenergetic parameters shown in the figure are: **(A)** non-mitochondrial respiration; **(B)** basal respiration; **(C)** maximal respiration; **(D)** spare respiratory capacity; **(E)** proton leak; and **(F)** ATP production. Data are expressed as mean ± SE. $n = 29$ per group, * $P < 0.05$ (ZDFL vs. ZDFO).

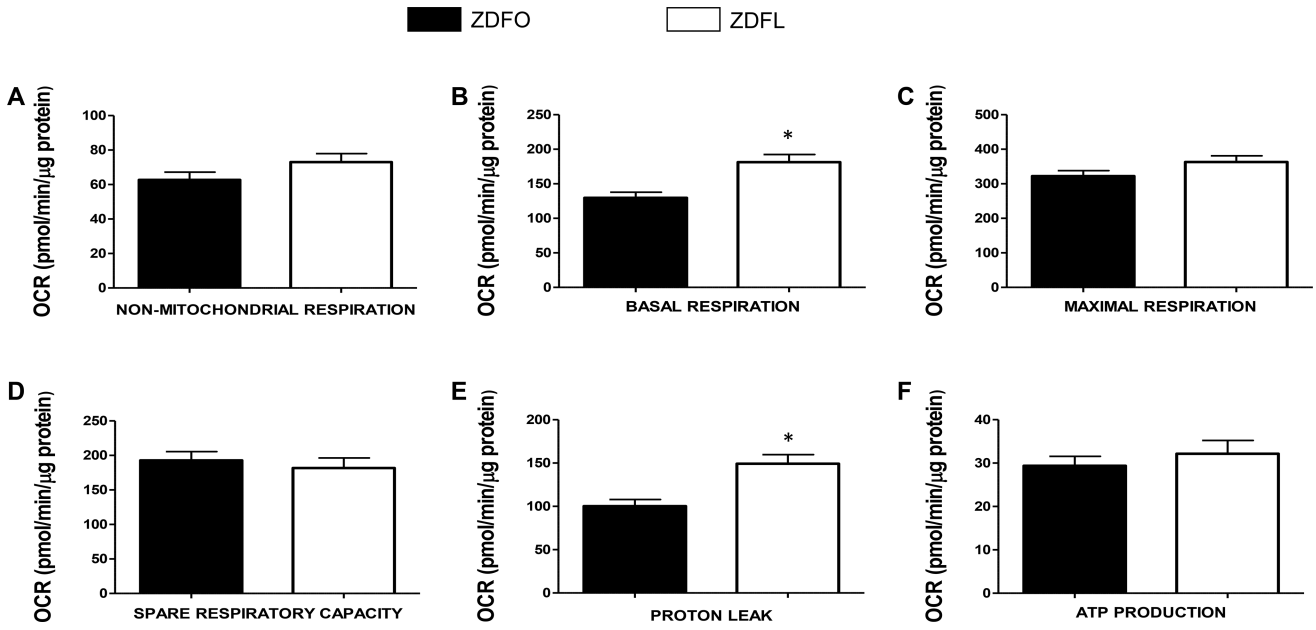

Figure 5. Mitochondrial respiration components of the large cerebral arteries, merged results

Mitochondrial bioenergetic parameters shown in the figure are: **(A)** non-mitochondrial respiration; **(B)** basal respiration; **(C)** maximal respiration; **(D)** spare respiratory capacity; **(E)** proton leak; and **(F)** ATP production. Data are expressed as mean ± SE. $n = 59$ per group. * $P < 0.05$ (ZDFL vs. ZDFO).

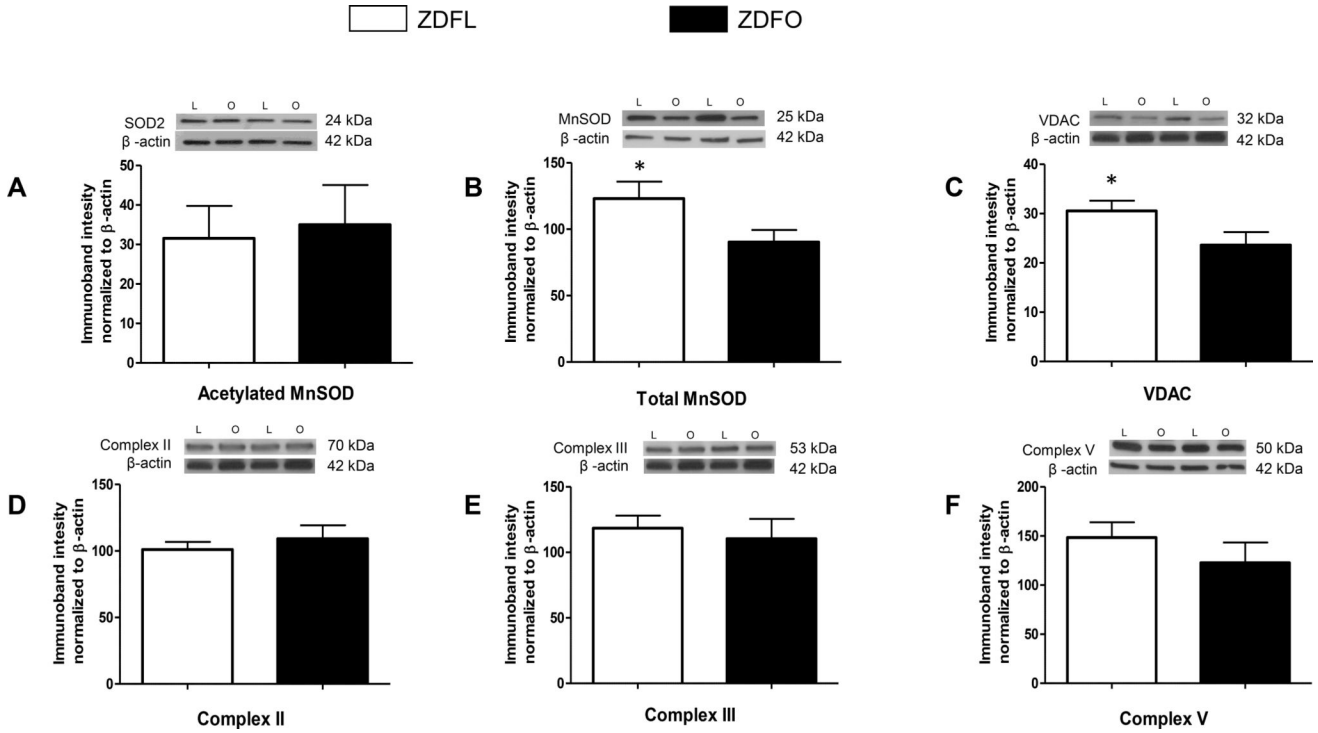

Figure 6. Mitochondrial protein expression in cerebral microvessels of ZDFL and ZDFO rats

Representative western blots and summary data: **(A)** Acetylated MnSOD, 24kDa; **(B)** total MnSOD, 25 kDa; **(C)** VDAC, 32 kDa; **(D)** Complex II, 70 kDa; **(E)** Complex III, 53 kDa; **(F)** Complex V, 50 kDA. L = lean, O = obese. Data are expressed as mean ± SE. $n = 16$ per group. * $P < 0.05$ (ZDFL vs. ZDFO).

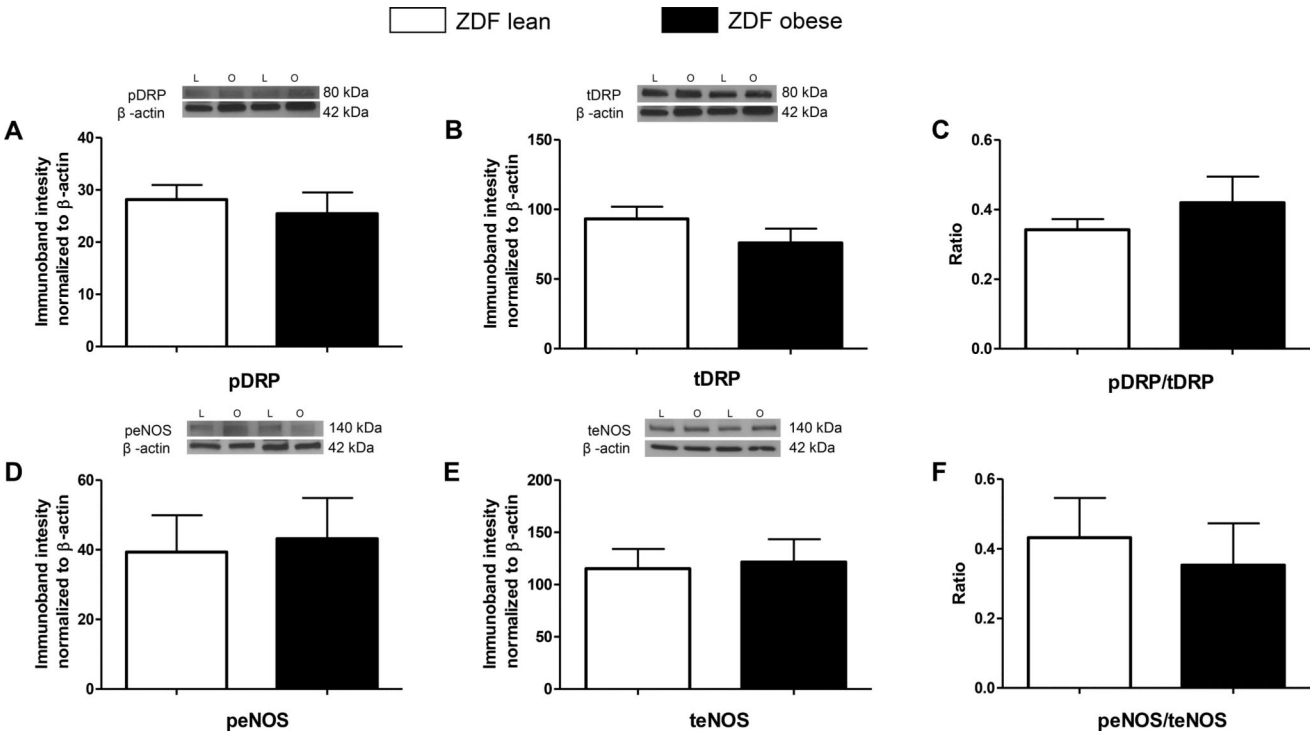

Figure 7. Mitochondrial and non-mitochondrial protein expression in cerebral microvessels of ZDFL and ZDFO rats

Representative western blots and summary data: **(A)** pDRP, 80 kDa; **(B)** tDRP, 80 kDa; **(C)** pDRP/tDRP ratio; **(D)** peNOS. 140 kDa; **(E)** teNOS, 140 kDa; **(F)** peNOS/teNOS ratio. L = lean, O = obese. Data are expressed as mean ± SE. *n* = 16 per group.

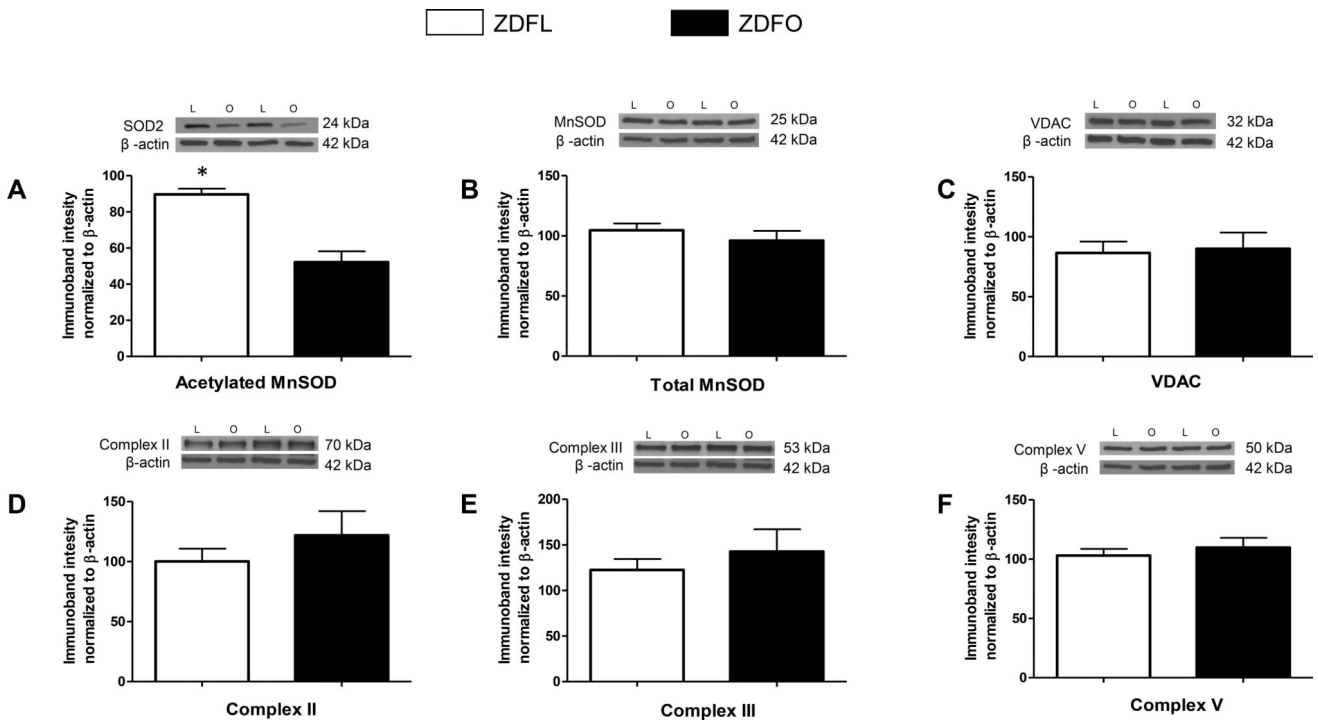

Figure 8. Mitochondrial protein expression in large cerebral arteries of ZDFL and ZDFO rats

Representative western blots and summary data: **(A)** Acetylated MnSOD, 24kDa; **(B)** total MnSOD, 25 kDa; **(C)** VDAC, 32 kDa; **(D)** Complex II, 70 kDa; **(E)** Complex III, 53 kDa; **(F)** Complex V, 50 kDA. L = lean, O = obese. Data are expressed as mean ± SE. $n = 16$ per group. * $P < 0.05$ (ZDFL vs. ZDFO).

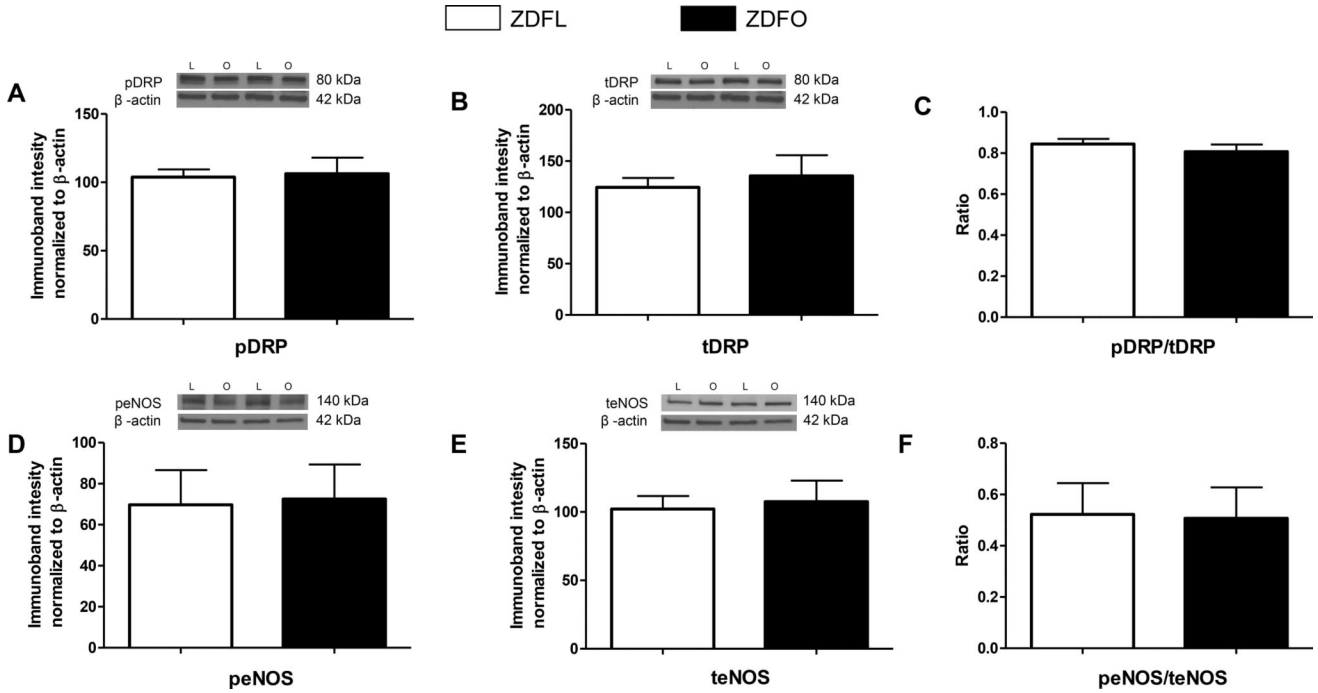

Figure 9. Mitochondrial and non-mitochondrial protein expression in large cerebral arteries of ZDFL and ZDFO rats

Representative western blots and summary data: **(A)** pDRP, 80 kDa; **(B)** tDRP, 80 kDa; **(C)** pDRP/tDRP ratio; **(D)** peNOS. 140 kDa; **(E)** teNOS, 140 kDa; **(F)** peNOS/teNOS ratio. L = lean, O = obese. Data are expressed as mean ± SE. n = 16 per group.

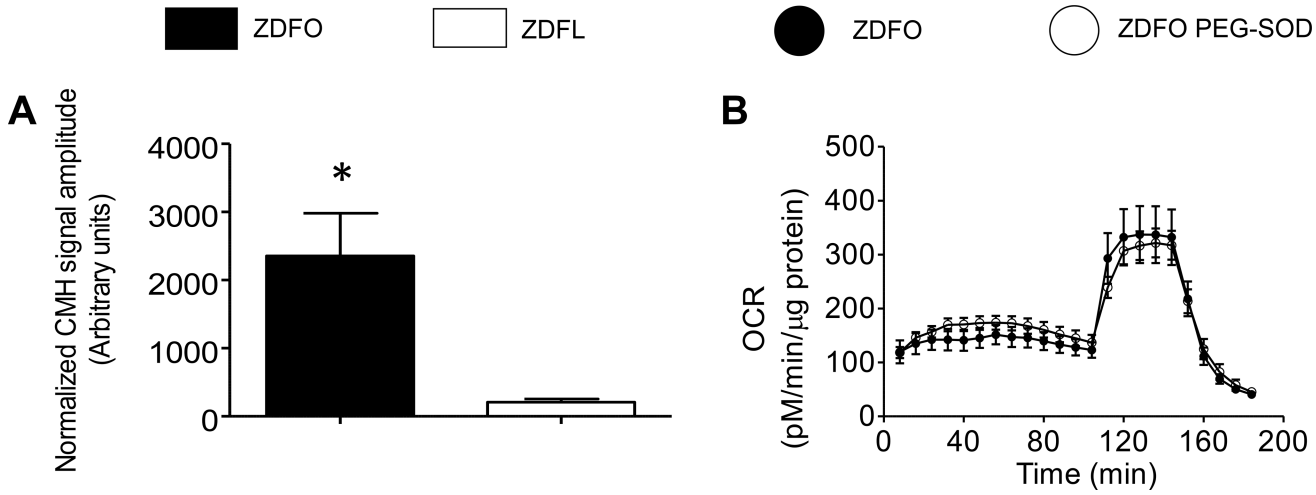

Figure 10. Superoxide levels in cerebral microvessels of ZDF rats and the effect of PEG-SOD on mitochondrial respiration profile

(A) Superoxide levels were significantly increased in the microvessels of ZDFO group compared with the ZDFL. $n = 10$, $P < 0.05$ (ZDFL vs. ZDFO). **(B)** Treatment with PEG-SOD did not ameliorate mitochondrial respiration in ZDFO group.